

Electronic Supporting Information

A new Aggregation Induced Emission Enhancement (AIEE) Dye which Self-assembles to Panchromatic Fluorescent Flowers and has Application in Sensing Dichromate ions

Vivekshinh Kshtriya^[a], Bharti Koshti^[a], Tahir Mehmood^[a], Ramesh Singh^[b], Khashti Ballabh
Joshi^[b], Sujoy Bandyopadhyay^[a], Danil W. Boukhvalov^[c,d], J. Prakasha Reddy^{[a]*}, Nidhi
Gour^{[a]*}

[a] Department of Chemistry, Indrashil University, Kadi, Mehsana, Gujarat, 382740, India;

E-mail: nidhi.gour@indrashiluniversity.edu.in; j.prakashareddy@gmail.com;
gournidhi@gmail.com

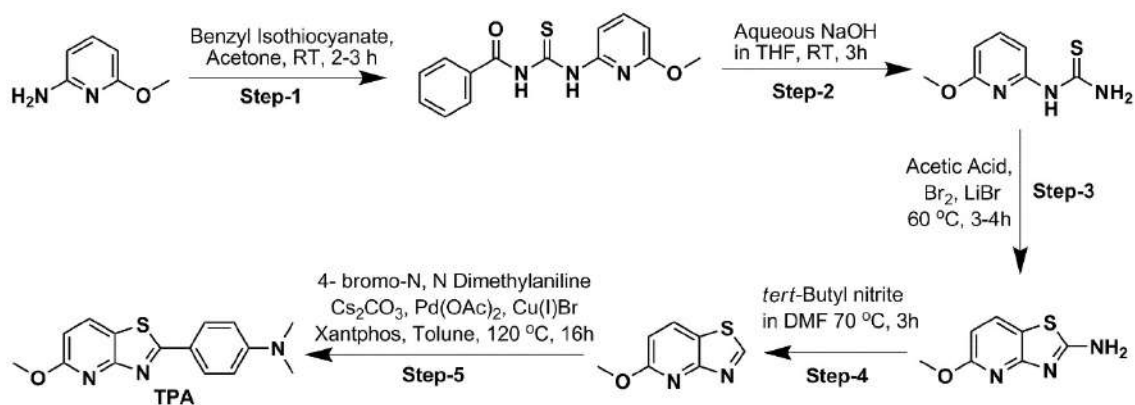
[b] Department of Chemistry, Dr. Harisingh Gour Vishwavidyalaya (A Central University)
Sagar, Madhya Pradesh, 470003, India;

[c] College of Science, Nanjing Forestry University, 159 Longpan Road, Nanjing 210037, PR
China;

[d] Institute of Physics and Technology, Ural Federal University, Mira Str. 19, 620002
Yekaterinburg, Russia

Synthesis of TPA: -

The synthesis of TPA is presented in scheme S1. The synthesis was done by using previously reported procedures and protocols in five steps.¹



Scheme S1 Synthetic routes of TPA and other intermediate compounds

Synthesis of Stage-1: A three-necked round bottom flask was fitted with a dropping funnel which contained 60 mL of dry acetone. A 5.0 g (27 mM) of 2-amino-6-methoxy pyridine was added in the round bottom flask and dropwise addition of dry acetone was done under nitrogen atmosphere from the addition funnel with constant and vigorous stirring of the reaction mixture. Subsequently, 6.9 g (42 mM) of benzoyl isothiocyanate was added and the reaction mixture was then allowed to stir for 2 to 4 hours at room temperature. The reaction was monitored by using analytical TLC and ethyl acetate: hexane (30%) solvent mixture as a mobile phase. After the completion of reaction, the reaction mixture was allowed to distill under reduced pressure to remove acetone. The residue was then poured carefully with stirring into 500 mL of cold water and the resulting yellow precipitate of (N-((6-methoxypyridin-2-yl)carbamothioyl)benzamide) was separated by suction filtration followed by washing of the precipitate with water (3 x 100 mL). The filtrate was further distilled under reduced pressure which yielded desired product (11 g, 36 mM, yield: 88%) as solid light-yellow material. M.P. 136 °C, Rf 0.53 (This material was used in the next step without any further purification).

Synthesis of stage-2: To the 20 mL THF solution of stage-1 (11 g) in three necked round bottom flask, 20 mL of aqueous NaOH (3.0 eq.) solution was added dropwise during the course of 15 minutes. The reaction mixture was then allowed to heat at 60 °C for 2-8 hours. The progress of the reaction was monitored by using TLC with the use of ethyl acetate: hexane (20%) solvent mixture as a mobile phase. After completion of the reaction the reaction mixture was distilled under reduced pressure and the residue was re-dissolved in ethyl acetate followed by extraction and washing with water and brine solution. Subsequently, to the organic layer, anhydrous sodium sulphate was added. The organic layer was then filtered and the solvent was evaporated using the high vacuum which gives intermediate-B (5.1 g, 27 mM, Yields 80%). The compound was then characterized by ¹H-NMR and used for the next step without any further purification. M.P. 214 °C, Rf 0.42, ¹H NMR (400 MHz, DMSO-*d*₆, 25°C, TMS) δ (ppm) = 10.50 (s, 1H), 10.04 (s, 1H), 8.85 (s, 1H), 7.68 (d, *J* = 8.0 Hz, 1H), 6.76 (d, *J* = 7.6Hz, 1H), 6.48 (t, *J* = 8.0 Hz, 1H), 3.71 (s, 3H).

Synthesis of Stage-3: Stage-2 (5.0 g, 2.73 mM, 1.0 eq.) was dissolved in acetic acid (30 mL) and stirred till the reaction mass becomes clear. Lithium bromide (4.6 g, 5.43 mM, 2.0 eq.) was added at room temperature and allowed to stirred it for 30 minutes. After that bromine (0.86 g, 50.00 mM, 2.0 eq.) was added at room temperature and the reaction mixture further stirred for 30 minutes. The reaction mixture was then refluxed at 60 °C for 4 to 8 hours. TLC observation in 50% ethyl acetate: hexane as a mobile phase showed that the starting material was consumed and product was formed. The reaction mixture was then allowed to cool at room temperature followed by the addition of 25% aqueous ammonia under ice cold condition to get pH 7 to 8. The crude solution was then extracted with (3 x 100 mL) ethyl acetate followed by washing with 10% NaHCO₃ solution (3 x 25 mL). The organic layer was then washed with brine solution (2 x 10 mL) followed by drying over anhydrous sodium sulphate. Ethyl acetate was evaporated under reduced pressure to get the crude compound,

which was further purified by using a silica gel column chromatography and 0-15% ethyl acetate and hexane as mobile phase which give (2.2 g, 11 mM, Yield: 65%), M.P. 174 °C, Rf 0.38, ¹H NMR (400 MHz, DMSO-*d*₆, 25°C, TMS) δ(ppm) = 7.38 (d, *J* = 8.4Hz, 1H), 6.54 (d, *J* = 8.4 Hz, 1H), 5.50 (s, 2H), 3.98 (s, t 3H). LC-MS for C₇H₉N₃OS was calculated 182.0388 and found [M+H]⁺ = 182.0399.

Synthesis of Stage-4: Take the stage-3 compound (1.0 g, 5.2 mM, 1.0 eq.) in THF and then tert-Butyl nitrite (1.1 g, 11.5 mM, 1.8 eq.) was added at room temperature. The reaction mixture was then refluxed at 60 °C for 12 hours. The progress of the reaction mixture was monitored by analytical TLC using 30% ethyl acetate: hexane mixture as a mobile phase which showed the starting material was completely consumed and the product was formed. The reaction mixture was then allowed to cool at room temperature. Ice cold water was added in the reaction mixture and extracted with (3 x 100 mL) ethyl acetate. The combine organic layer was collected and washed with the saturated brine solution (3 x 10 mL) followed by drying of the organic layer over anhydrous sodium sulphate. Ethyl acetate was evaporated to get the crude compound (1.5 g), which was further purified by using a silica gel column chromatography in (0 to 20% ethyl acetate gradient in hexane) to give (2.5 g, yield: 70%, M.P. 99 °C), Rf 0.6, ¹H NMR (400 MHz DMSO-*d*₆, 25 °C, TMS) δ(ppm)= 9.55 (s, 1H); 8.5 (d, *J* = 8.8 Hz, 1H); 6.96 (d, *J* = 8.8 Hz, 1H); 3.93(s, 3H). ¹³C NMR (100 MHz, DMSO-*d*₆, 25 oC, TMS) δ(ppm) = 170.13, 162.86, 142.00, 132.18, 116.12, 103.09, 53.40. LCHRMS for C₇H₈N₂OS was calculated 167.0279 and found [M+H]⁺ = 167.0282.

Synthesis of TPA: Stage-4 (0.5 g, 3.0 mM, 1.0 eq.), 4-Bromo-*N,N*-dimethylaniline (0.602 g, 3.0 mM, 1.0 eq.) and cesium carbonate (Cs₂CO₃) (2.94 g, 9.01 mM, 3.0 eq.) was taken in a pressure vial and subsequently dissolved it in toluene (10 mL). The reaction mixture was degassed for 15 minute at room temperature. Copper(I)bromide (Cu(I)Br) (0.346 g, 2.408 mM, 1.0 eq.), palladium (II) acetate (Pd(OAc)₂) (0.169 g, 0.6 mM, 1 eq.) and xantphos (0.7 g,

1.0 mM, 0.3 eq.) was added and then the reaction mixture was further degassed for another 5 minutes. The reaction mixture was then sealed in pressure vial and again heated at 120 °C for 16 hours. After the completion of the reaction, the reaction mixture was allowed to cool at room temperature and the reaction mass was dried under reduced pressure and the remaining residue poured into the ice-cold water followed by the extraction with (3 x 100 mL) ethyl acetate. The combined organic layer was collected and washed with saturated brine solution (1 x 10 mL), followed by drying of the organic layer over anhydrous sodium sulphate. Ethyl acetate was evaporated under reduced pressure to get the crude compound (0.7 g) which was further purified by using a silica gel column chromatography in (0 to 30% ethyl acetate gradient in hexane) to give a yellow color solid. (0.2 g), R_f 0.49, ¹H NMR: (400 MHz, DMSO-*d*₆, 25°C, TMS) δ (ppm) = 8.36 (d, *J*=8.00 Hz, 1H); 7.93-7.90 (m, 2H); 8.12 (dd, 3H); 3.98 (s, 3H); 3.04(s, 6H); ¹³C NMR (400 MHz, DMSO-*d*₆, 25 °C, TMS) δ(ppm)= 171.23, 163.55, 163.04, 152.98, 133.81, 128.70, 120.45, 119.98, 112.26, 108.24, 53.84, 40.65 LC-MS for C₁₅H₁₅N₃OS was calculated 285.09 and found [M+H]⁺ = 286.39.



Fig. S2 TLC and vial image of **TPA** under UV chamber.

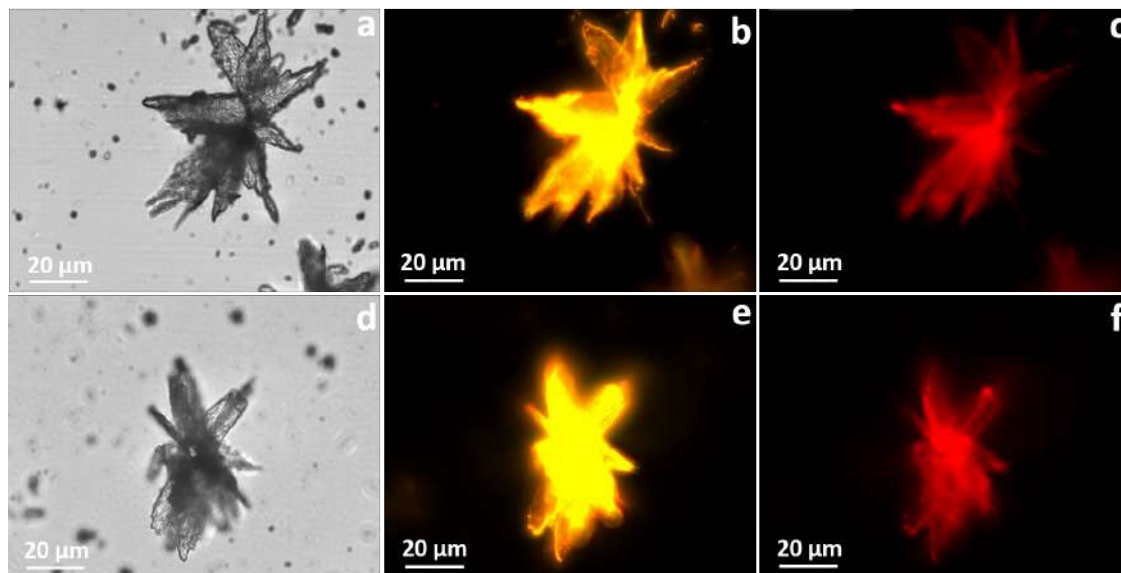


Fig S3 Microscopic images of **TPA** (3 mM) after 24 h of incubation at RT in DMSO (a) Optical microscopy image under bright field; (b) Fluorescence microscopy image under FITC filter (Ex 480/40; Em 527/30); (c) Fluorescence microscopy image under rhodamine filter (Ex 546/10; Em 585/40). Microscopic images of **TPA** in DMSO (3 mM) incubated for 1 h at 37.4 °C (d) Optical microscopy image under bright field; (e) Fluorescence microscopy image under FITC filter (Ex 480/40; Em 527/30); (f) Fluorescence microscopy image under rhodamine filter (Ex 546/10; Em 585/40).

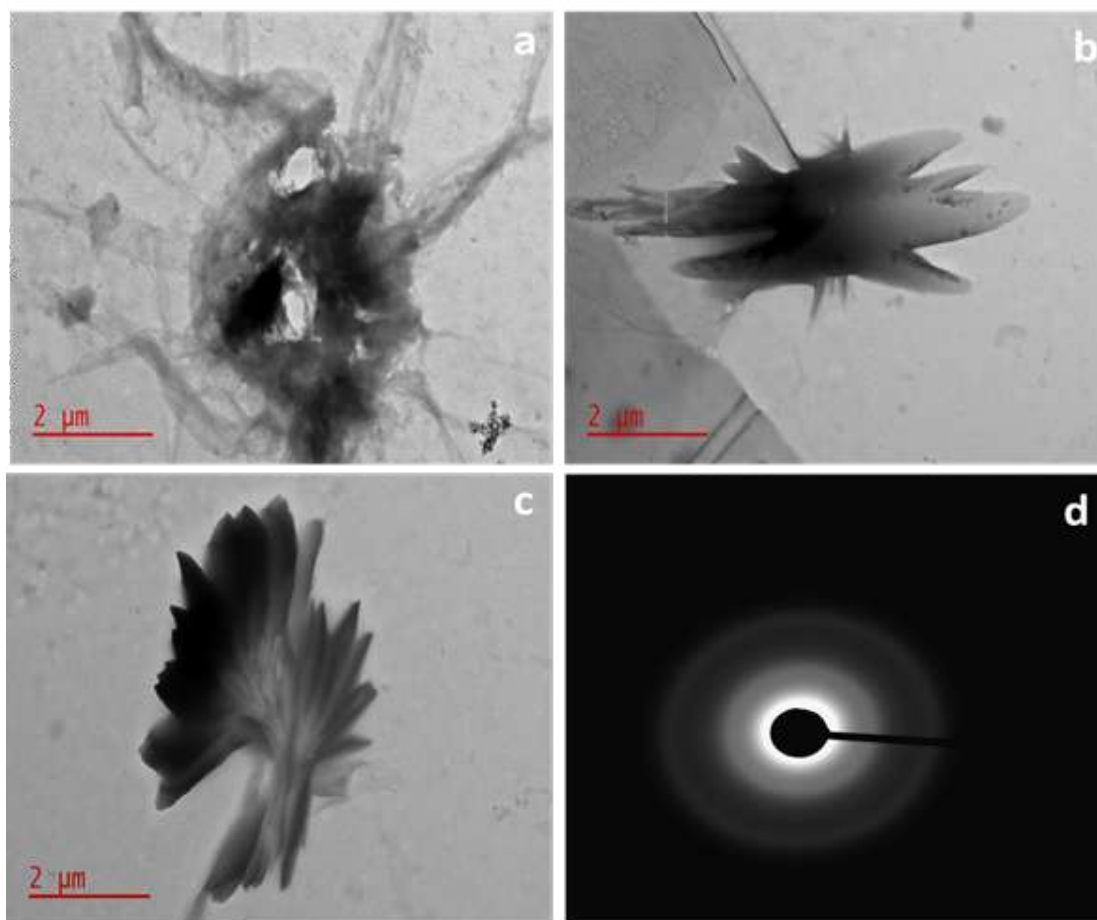


Fig. S4 Transmission electron microscopy (TEM) images of TPA in DMSO (a-c) at 2 μm ; (d) Selected area electron diffraction of TPA reveal it is not crystalline in nature.

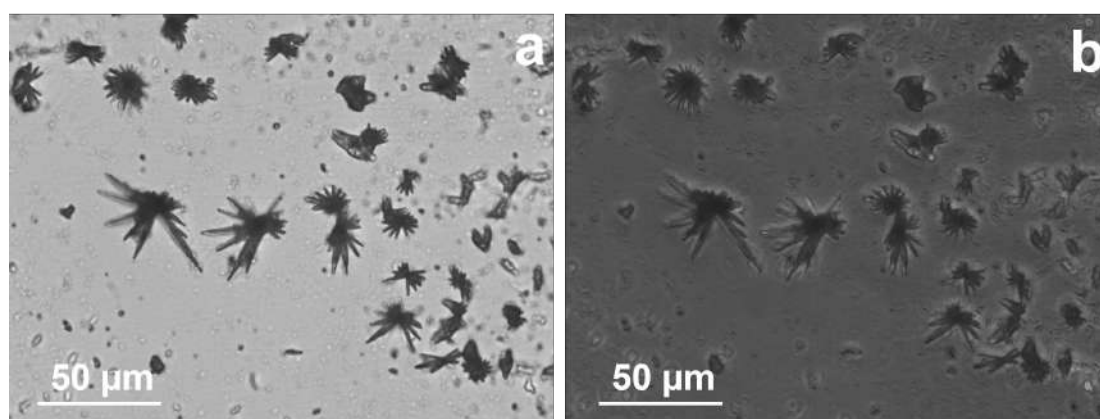


Fig. S5 Optical microscopy images of TPA (a) Under bright field; (b) Phase contrast image of TPA confirm non crystalline nature as the structures appeared dark and not shiny.

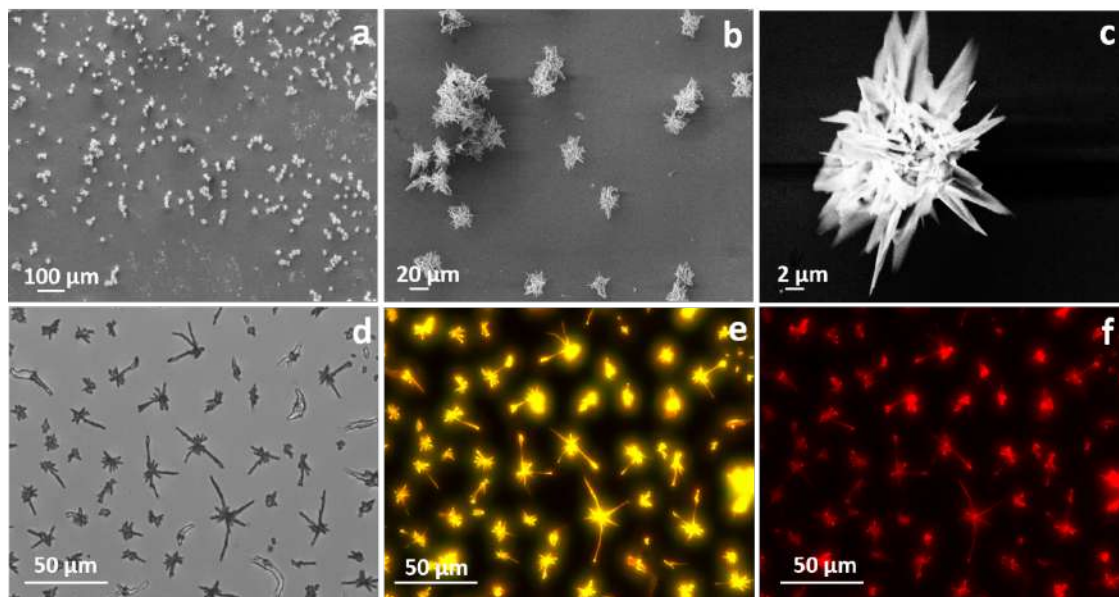


Fig. S6 Microscopic images of **TPA** in THF (3 mM) incubated for 1 h at 25 °C (a-c) SEM images under different magnifications; (d) Optical microscopy image under bright field; (e) Fluorescence microscopy image under FITC filter (Ex 480/40; Em 527/30); (f) Fluorescence microscopy image under rhodamine filter (Ex 546/10; Em 585/40).

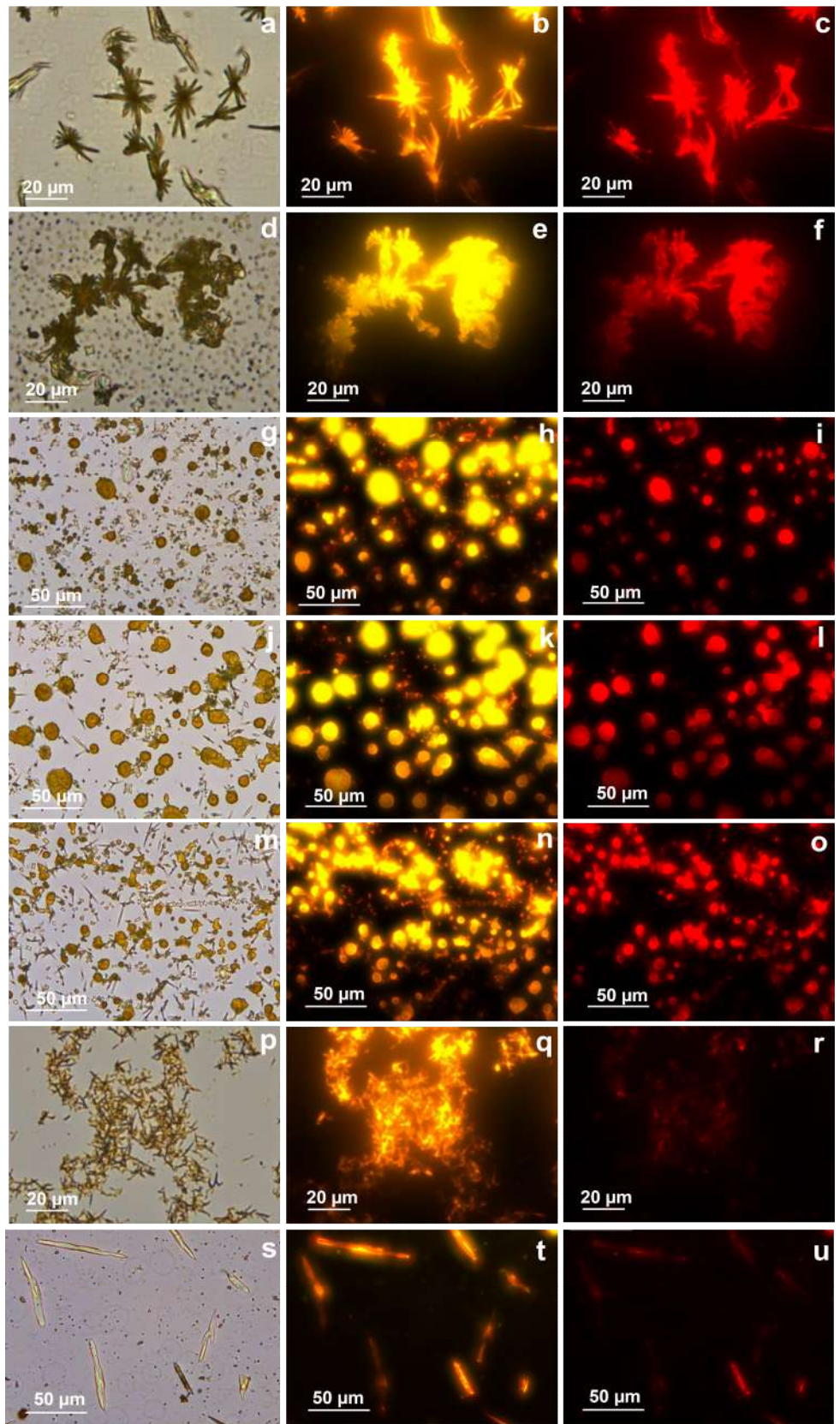


Fig. S7 Microscopic images of TPA under the varying percentage of water in THF under bright field, FITC filter (Ex 480/40; Em 527/30) and rhodamine filter (Ex 546/10; Em 585/40) (a-c) TPA assembles to flower-like structures in neat THF; (d-f) gradually starts aggregating at 10% water in THF; (g-i) as the percentage of water in THF is increased to 30%; (j-l) morphological transitions could be observed with spherical aggregates which become more aggregated at 50% water in THF; (m-o) more aggregated spherical are observed till 70% water in THF; (p-r) disaggregates to small rods and small particles at 90% water in THF which is accompanied by a decrease in the fluorescence; (s-u) shows crystalline rod-like structure in 98% water in THF.



Fig. S8 The vial images of TPA with increasing % of water in DMSO from 0-98 % water. (Under UV transillumination ~320 nm)

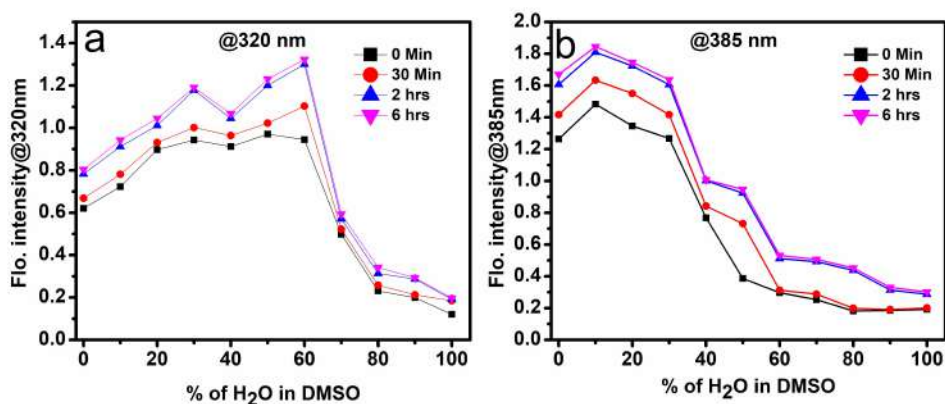


Fig. S9 The graph of intensity of fluorescence of TPA vs percentage of water in DMSO (a) recorded at Ex 320 in different time intervals from 0-6 h; (b) recorded at Ex 385 in different time intervals from 0-6 h

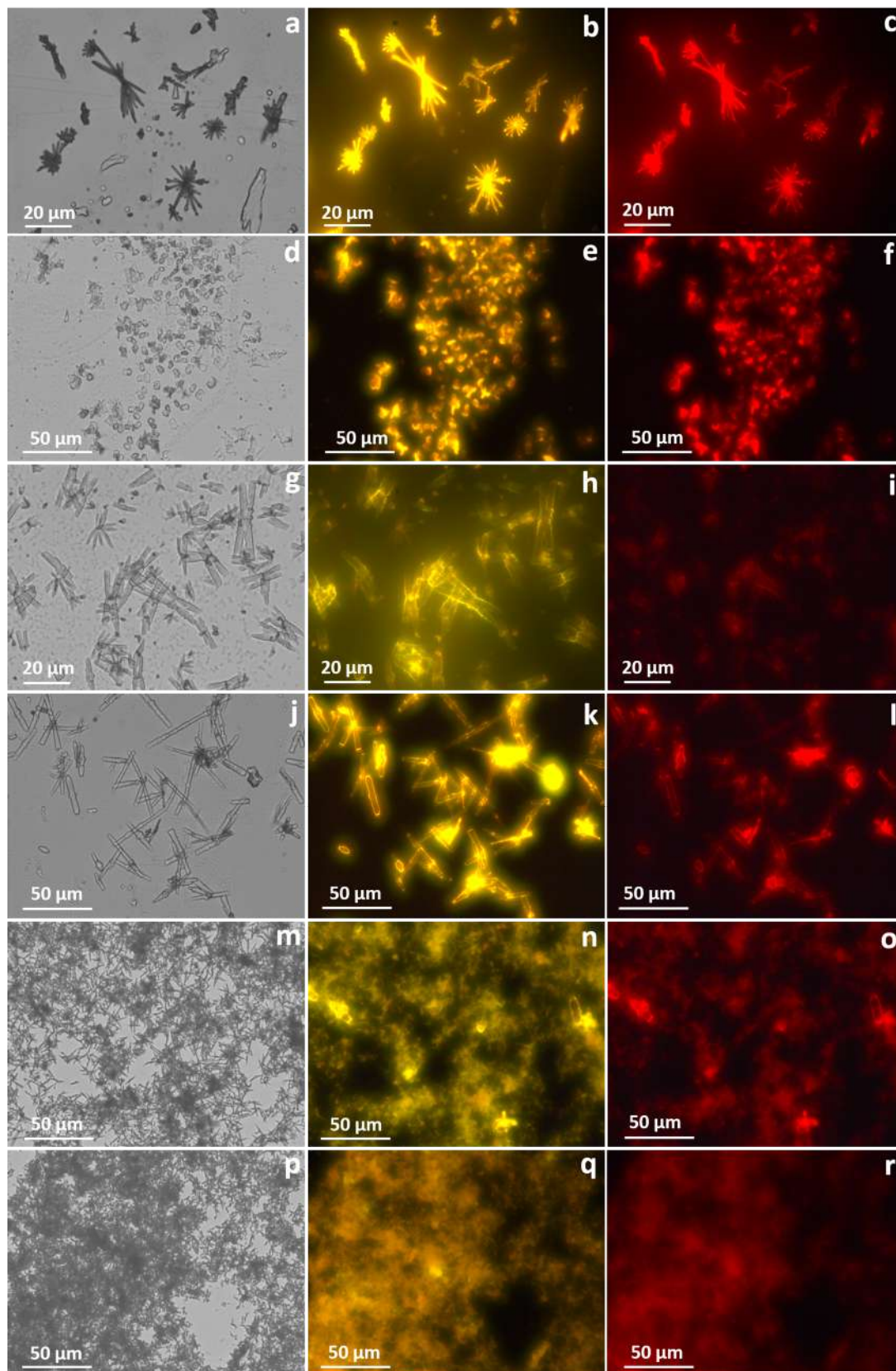


Fig. S10 Microscopic images of TPA under the varying percentage of water in acetone under

bright field, FITC filter (Ex 480/40; Em 527/30) and rhodamine filter (Ex 546/10; Em 585/40). (a-c) in neat acetone; (d-f) at 10% water in acetone; (g-i) at 30% water in acetone; (j-l) at 50% water in acetone; (m-o) at 70% water in acetone; (p-r) at 90% water in acetone.

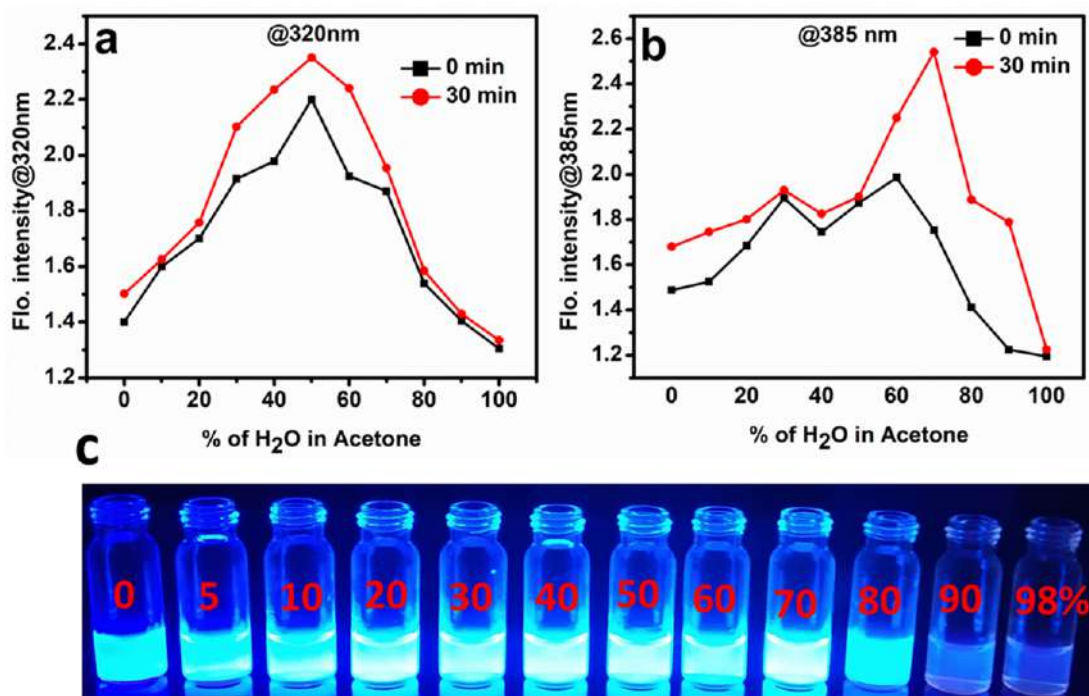


Fig. S11 The graph of the intensity of fluorescence of TPA vs percentage of water in acetone (a) at Ex 320 before and after 30 minutes; (b) at Ex 385 before and after 30 minutes; (c) Vial images of TPA in acetone with increasing percentage of water from 0 to 98% under UV light (~320 nm).

HOMO LUMO calculations

The HOMO and LUMO energy calculation have been carried out by using B3LYP (Becke three-parameter Lee-Yang-Parr). Further the molecular geometric structure of TPA has been optimized by DFT calculations subsequently the energy calculations were done and the optimized structure has been shown in Fig. S12 and S13.

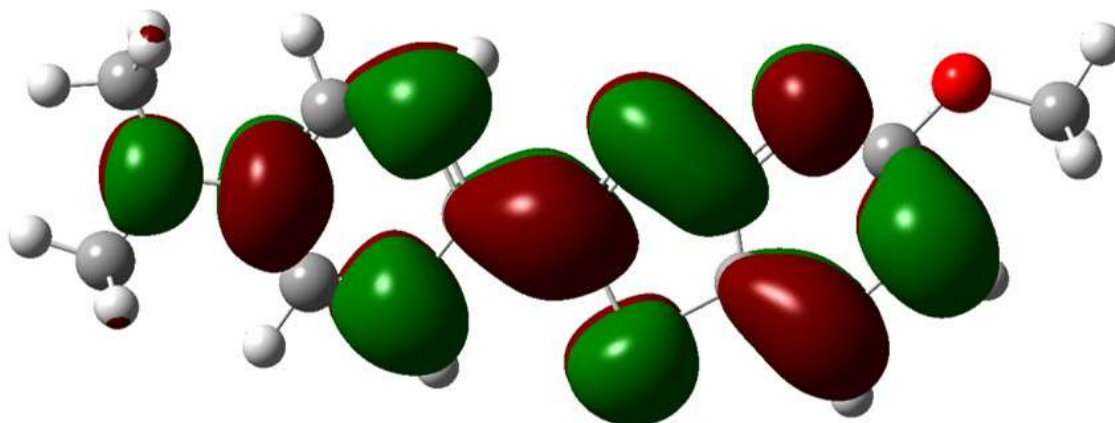


Fig. S12 Lowest unoccupied molecular orbital (LUMO) diagram

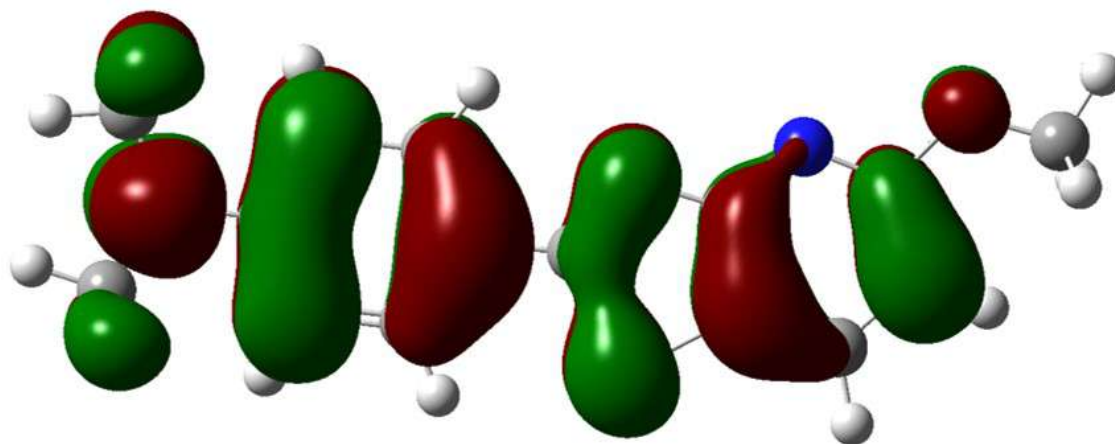


Fig. S13 Highest occupied molecular orbital (HOMO) diagram

Fig. S14 Calculated binding energies in eV (first set) and probabilities calculated by Boltzmann formula at room temperature for two TPA molecules connected by single water molecule (see Fig. 5a, 5b in main text). The zero angle is corresponding with head over head configuration and 180 degree with head over tail configuration.

Degree / Binding Energy (eV)

| | |
|----|---------|
| 0 | -0,2451 |
| 10 | -0,6844 |
| 20 | -0,8206 |
| 30 | -0,7506 |
| 40 | -0,6792 |
| 50 | -0,6096 |
| 60 | -0,6149 |
| 70 | -0,6883 |

80 -0,6386
90 -0,6801
100 -0,2599
110 -0,1564
120 -0,8375
130 -0,8491
140 -0,9588
150 -0,6152
160 -0,3346
170 -0,1283
180 -0,1455
190 -0,1283
200 -0,3346
210 -0,6152
220 -0,9588
230 -0,8491
240 -0,8375
250 -0,1564
260 -0,2599
270 -0,6801
280 -0,6386
290 -0,6883
300 -0,6149
310 -0,6096
320 -0,6792
330 -0,7506
340 -0,8206
350 -0,6844

Degree / Probability (%)

| | |
|------------|----------------|
| 0.0000000 | 4.14047650E-11 |
| 10.0000000 | 1.11283641E-03 |
| 20.0000000 | 0.223782480 |
| 30.0000000 | 1.46553339E-02 |
| 40.0000000 | 9.08844173E-04 |
| 50.0000000 | 6.04538836E-05 |
| 60.0000000 | 7.43116325E-05 |
| 70.0000000 | 1.29535247E-03 |
| 80.0000000 | 1.87011217E-04 |
| 90.0000000 | 9.41261707E-04 |
| 100.000000 | 7.36793335E-11 |
| 110.000000 | 1.30908479E-12 |
| 120.000000 | 0.432151675 |
| 130.000000 | 0.678913713 |
| 140.000000 | 48.6458473 |
| 150.000000 | 7.51847256E-05 |
| 160.000000 | 1.35101985E-09 |
| 170.000000 | 4.38272763E-13 |
| 180.000000 | 8.56305315E-13 |

| | |
|------------|----------------|
| 190.000000 | 4.38272763E-13 |
| 200.000000 | 1.35101985E-09 |
| 210.000000 | 7.51847256E-05 |
| 220.000000 | 48.6458473 |
| 230.000000 | 0.678913713 |
| 240.000000 | 0.432151675 |
| 250.000000 | 1.30908479E-12 |
| 260.000000 | 7.36793335E-11 |
| 270.000000 | 9.41261707E-04 |
| 280.000000 | 1.87011217E-04 |
| 290.000000 | 1.29535247E-03 |
| 300.000000 | 7.43116325E-05 |
| 310.000000 | 6.04538836E-05 |
| 320.000000 | 9.08844173E-04 |
| 330.000000 | 1.46553339E-02 |
| 340.000000 | 0.223782480 |
| 350.000000 | 1.11283641E-03 |

Fig. S15 Calculated binding energies in eV (first set) and probabilities calculated by Boltzmann formula at room temperature for two **TPA** molecules without solvent molecules between (see Figure 5c, 5d, 5e and 5f in main text). The zero angle is corresponding with head over head configuration and 180 degree with head over tail configuration.

Degree / Binding Energy (eV)

| | |
|-----|----------|
| 0 | -0,67155 |
| 10 | -0,64485 |
| 20 | -0,67265 |
| 30 | -0,66105 |
| 40 | -0,61385 |
| 50 | -0,5852 |
| 60 | -0,5778 |
| 70 | -0,57 |
| 80 | -0,54 |
| 90 | -0,3642 |
| 100 | -0,66125 |
| 110 | -0,6447 |
| 120 | -0,63755 |
| 130 | -0,64445 |
| 140 | -0,5157 |
| 150 | -0,5005 |
| 160 | -0,4733 |
| 170 | -0,66125 |
| 180 | -0,65195 |
| 190 | -0,66125 |
| 200 | -0,6447 |
| 210 | -0,63755 |
| 220 | -0,64445 |

230 -0,5157
240 -0,5005
250 -0,4733
260 -0,4823
270 -0,3642
280 -0,54
290 -0,57
300 -0,5778
310 -0,5852
320 -0,61385
330 -0,66105
340 -0,67265
350 -0,64485

Degree / Probability (%)

| | |
|------------|----------------|
| 0.0000000 | 10.0793095 |
| 10.0000000 | 3.56356144 |
| 20.0000000 | 10.5204401 |
| 30.0000000 | 6.69664383 |
| 40.0000000 | 1.06565535 |
| 50.0000000 | 0.349214226 |
| 60.0000000 | 0.261784434 |
| 70.0000000 | 0.193210810 |
| 80.0000000 | 6.00724779E-02 |
| 90.0000000 | 6.39102072E-05 |
| 100.000000 | 6.74898577 |
| 110.000000 | 3.54280329 |
| 120.000000 | 2.68180799 |
| 130.000000 | 3.50848770 |
| 140.000000 | 2.33193990E-02 |
| 150.000000 | 1.29020195E-02 |
| 160.000000 | 4.47357260E-03 |
| 170.000000 | 6.74898577 |
| 180.000000 | 4.69849396 |
| 190.000000 | 6.74898577 |
| 200.000000 | 3.54280329 |
| 210.000000 | 2.68180799 |
| 220.000000 | 3.50848770 |
| 230.000000 | 2.33193990E-02 |
| 240.000000 | 1.29020195E-02 |
| 250.000000 | 4.47357260E-03 |
| 260.000000 | 6.35128375E-03 |
| 270.000000 | 6.39102072E-05 |
| 280.000000 | 6.00724779E-02 |
| 290.000000 | 0.193210810 |
| 300.000000 | 0.261784434 |
| 310.000000 | 0.349214226 |
| 320.000000 | 1.06565535 |
| 330.000000 | 6.69664383 |

| | |
|------------|------------|
| 340.000000 | 10.5204401 |
| 350.000000 | 3.56356144 |

Fig. S16 Calculated binding energies in eV (first set) and probabilities calculated by Boltzmann formula at room temperature for two TPA molecules with DMSO solvent molecules between (see Figure 5g, 5h in main text). The zero angle is corresponding with head over head configuration and 180 degree with head over tail configuration.

Degree / Binding Energy (eV)

| | |
|-----|---------|
| 0 | -1,1649 |
| 10 | -1,1110 |
| 20 | -1,1250 |
| 30 | -1,1445 |
| 40 | -1,1580 |
| 50 | -1,0365 |
| 60 | 0,8889 |
| 70 | 1,2969 |
| 80 | 1,7962 |
| 90 | 1,8061 |
| 100 | 1,8901 |
| 110 | 1,9408 |
| 120 | 0,7755 |
| 130 | 1,3711 |
| 140 | 1,6600 |
| 150 | 1,8696 |
| 160 | 1,4670 |
| 170 | 2,0065 |
| 180 | 1,9327 |
| 190 | 2,0065 |
| 200 | 1,4670 |
| 210 | 1,8696 |
| 220 | 1,6600 |
| 230 | 1,3711 |
| 240 | 0,7755 |
| 250 | 1,9408 |
| 260 | 1,8901 |
| 270 | 1,8061 |
| 280 | 1,7962 |
| 290 | 1,2969 |
| 300 | 0,8889 |
| 310 | -1,0365 |
| 320 | -1,1580 |
| 330 | -1,1445 |
| 340 | -1,1250 |
| 350 | -1,1110 |

Degree / Probability (%)

| | |
|------------|----------------|
| 0.0000000 | 24.3070126 |
| 10.0000000 | 2.97976971 |
| 20.0000000 | 5.13984776 |
| 30.0000000 | 10.9832706 |
| 40.0000000 | 18.5798321 |
| 50.0000000 | 0.163775608 |
| 60.0000000 | 4.48901778E-34 |
| 70.0000000 | 5.65073606E-41 |
| 80.0000000 | 0.00000000 |
| 90.0000000 | 0.00000000 |
| 100.000000 | 0.00000000 |
| 110.000000 | 0.00000000 |
| 120.000000 | 3.71497005E-32 |
| 130.000000 | 3.14171116E-42 |
| 140.000000 | 0.00000000 |
| 150.000000 | 0.00000000 |
| 160.000000 | 7.56701171E-44 |
| 170.000000 | 0.00000000 |
| 180.000000 | 0.00000000 |
| 190.000000 | 0.00000000 |
| 200.000000 | 7.56701171E-44 |
| 210.000000 | 0.00000000 |
| 220.000000 | 0.00000000 |
| 230.000000 | 3.14171116E-42 |
| 240.000000 | 3.71497005E-32 |
| 250.000000 | 0.00000000 |
| 260.000000 | 0.00000000 |
| 270.000000 | 0.00000000 |
| 280.000000 | 0.00000000 |
| 290.000000 | 5.65073606E-41 |
| 300.000000 | 4.48901778E-34 |
| 310.000000 | 0.163775608 |
| 320.000000 | 18.5798321 |
| 330.000000 | 10.9832706 |
| 340.000000 | 5.13984776 |
| 350.000000 | 2.97976971 |

Table S1 Crystallographic data and refinement parameters for TPA crystal.

| Parameters | TPA |
|-------------------|--|
| Empirical formula | <u>C₁₅H₁₅N₃OS</u> |
| Formula weight | 285.36 |
| Temperature (K) | 294(2) |
| Crystal system | Monoclinic |
| Space group | <i>P</i> 2 ₁ / <i>n</i> |
| a, (Å) | 6.6492 (8) |
| b, (Å) | 13.731 (2) |
| c, (Å) | 15.329 (2) |

| | |
|---|--|
| β , ($^{\circ}$) | 101.032 (5) |
| Volume (\AA^3) | 1373.7 (3) |
| Z | 4 |
| μ (mm^{-1}) | 0.23 |
| $F(000)$ | 600 |
| Crystal size (mm^3) | $0.27 \times 0.24 \times 0.16$ |
| Radiation | MoK α ($\lambda = 0.71073$) |
| Index ranges | $-7 \leq h \leq 8, -18 \leq k \leq 18, -20 \leq l \leq 20$ |
| Reflections collected | 29104 |
| Independent reflections | 3402 [$R_{\text{int}} = 0.084$] |
| No. of parameters | 184 |
| Goodness-of-fit on F^2 | 1.075 |
| Final R indexes [$I \geq 2\sigma(I)$] | $R_1 = 0.1081, wR_2 = 0.1465$ |
| Final R indexes [all data] | $R_1 = 0.0623, wR_2 = 0.1279$ |
| Largest diff. peak/hole ($e \text{\AA}^{-3}$) | 0.19/-0.20 |
| CCDC deposition no. | 2109329 |

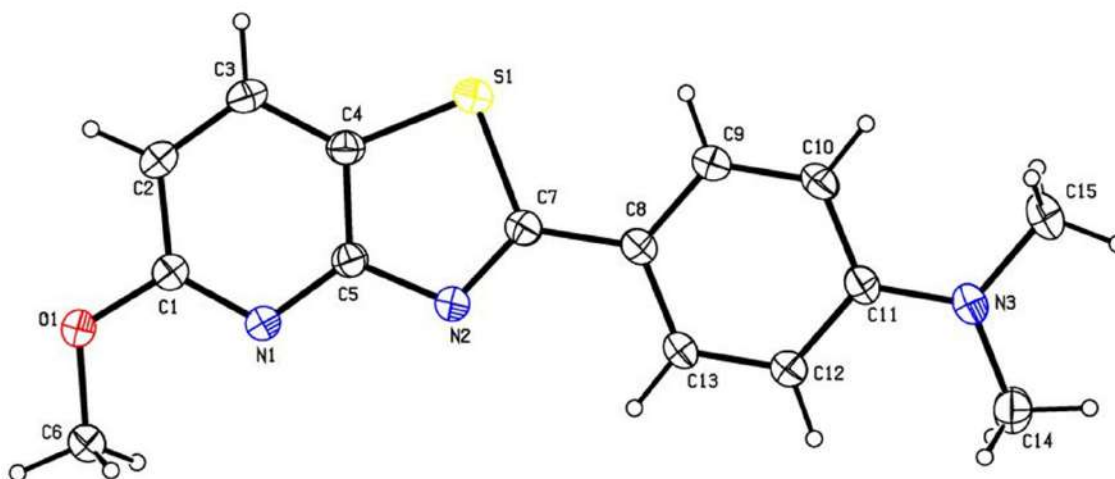


Fig. S17 View of TPA showing the atom-labelling scheme. Displacement ellipsoids are drawn at the 30% probability level and H atoms are represented by circles of arbitrary radii.

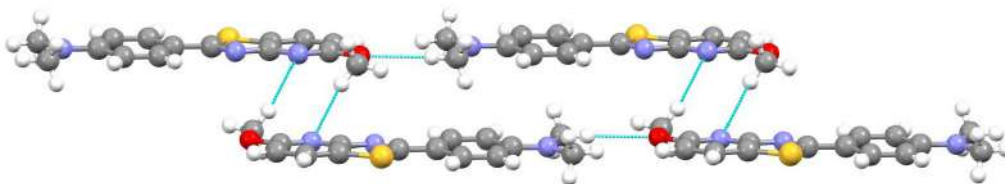


Fig. S18 Visualization of interactions between stacked layers through C-H...N hydrogen bonding.

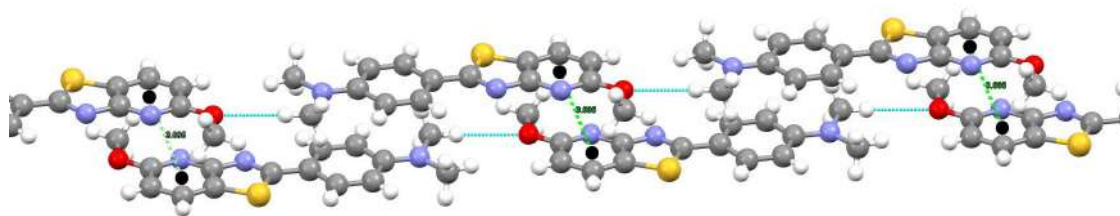


Fig. S19 Visualization of interactions between stacked layers through $\pi\cdots\pi$ (between pyridothiazole fragments) contacts.

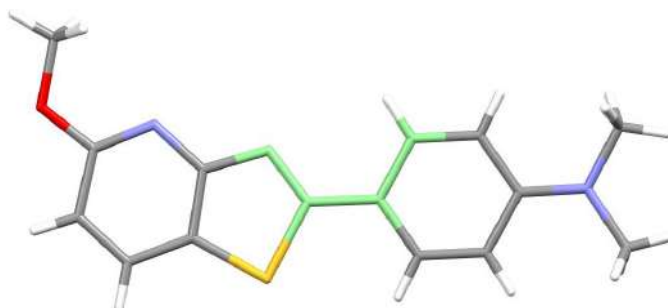


Fig. S20 Dihedral angle (torsion angle) along the C-C bond connecting methoxy benzothiazole fragment and dimethylaniline ring (highlighted in light green) of TPA.



Fig. S21 The vial images of TPA with increasing percentage of water in THF from 0-98 % water under day light.

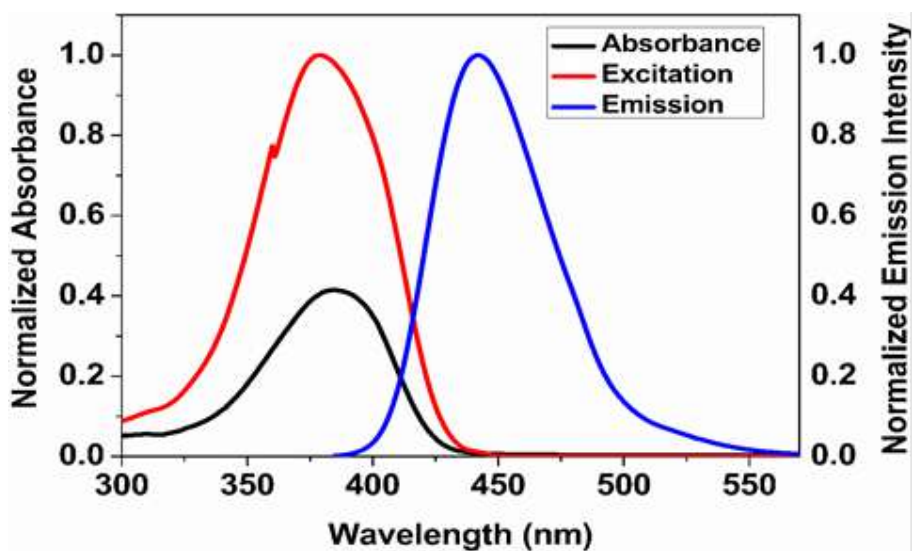


Fig. S22 Normalized absorption, emission ($\lambda_{ex} = 385 \text{ nm}$) and excitation ($\lambda_{em} = 452 \text{ nm}$) spectra of TPA at $10 \mu\text{M}$ concentration.

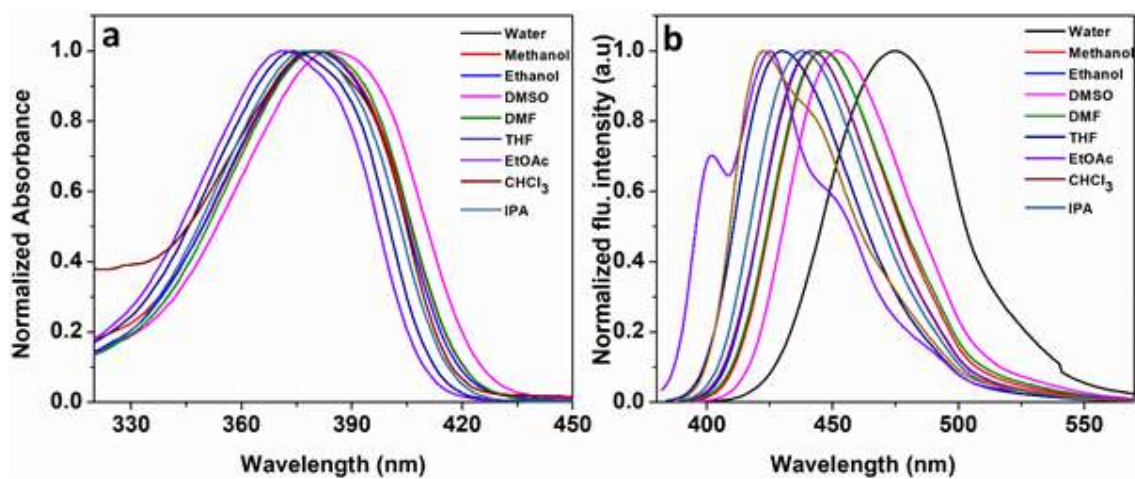


Fig. S23 UV and fluorescence spectra of TPA in various solvents (a) Normalized UV-Visible spectra of TPA in different solvents at $10 \mu\text{M}$ concentration; (b) Normalized fluorescence spectra of TPA in different solvents at $10 \mu\text{M}$ concentration.

Table S2 Spectroscopic data of **TPA** in various organic solvents.

| Solvent | Absorption | | Fluorescence |
|----------------------------|---|---|---|
| | λ_{max} (nm) TE region | λ_{max} (nm) PI region | λ_{max} (nm) |
| Water | 380 | 380 | 475 |
| Methanol | 381 | 381 | 446 |
| Ethanol | 380 | 380 | 441 |
| DMSO | 385 | 385 | 452 |
| DMF | 382 | 382 | 446 |
| Acetone | 377 | 377 | 437 |
| THF | 374 | 374 | 430 |
| Ethyl acetate | 372 | 372 | 425 |
| Acetonitrile | 385 | 385 | 442 |
| Chloroform | 379 | 379 | 423 |
| n-Hexane | 365 | 365 | 417 |
| Isopropyl alcohol (IPA) | 379 | 379 | 437 |

The photophysical properties of new **TPA** is summarised in Table S2.

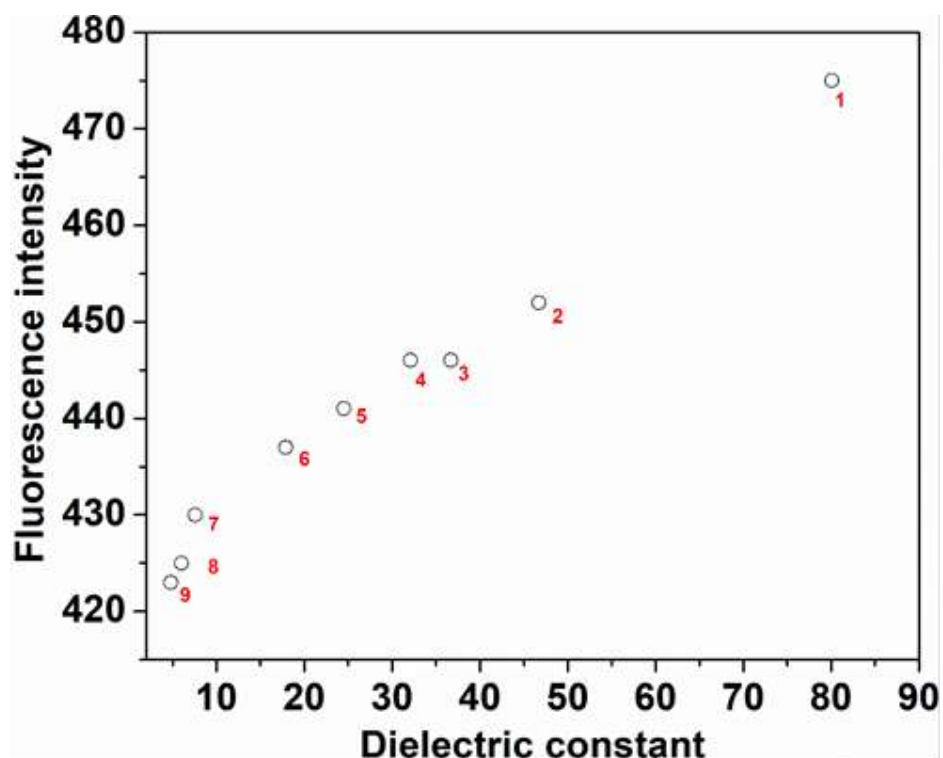


Fig. S24 Position of ellipticine fluorescence maximum as a function of solvent dielectric constants such as **1**(water), **2**(methanol), **3**(ethanol), **4**(DMSO), **5**(DMF), **6**(THF), **7**(EtOAc), **8**(CHCl₃), **9**(IPA).

Table S3 Fluorescence decay parameters for **TPA** in DMF; the lifetimes (τ_1 , τ_2 , and τ_3) and the respective fractional contributions (α_1 , α_2 and α_3), the weighted average lifetime (τ_{avg}) and the quality of fitting (χ^2) for the data in Fig. 7d are shown.

| Sample | τ_1 (ns) | α_1 | τ_2 (ns) | α_2 | τ_3 (ns) | α_3 | τ_{avg} (ns) | χ^2 |
|------------|---------------|------------|---------------|------------|---------------|------------|-------------------|----------|
| TPA | 0.66 | 49.42 | 1.75 | 1.12 | 0.66 | 49.47 | 0.668 | 1.53 |

Fluorescence quantum yield (Φ_{f}) measurement:

The fluorescence quantum yields of **TPA** in DMF were estimated by comparison with coumarin-153 in ethanol ($\Phi_f = 0.38$). (The quantum yields were calculated using the following equation.^{2,3})

$$\Phi_{f, x} = \Phi_{f, s} \cdot \frac{F_x}{F_s} \cdot \frac{f_s}{f_x} \cdot \frac{n_x^2}{n_s^2}$$

where, is fluorescence quantum $\Phi_{f, x}$ yield, subscript x denotes unknown sample and subscript s refers to standard. F denotes integral fluorescence; n refers to refractive index of the solvent used in the measurements and f is the absorption factor at the excitation wavelength given by the following equation:

$$f = 1 - 10^{-\epsilon(\lambda_{ex})cl} = 1 - 10^{-A(\lambda_{ex})}$$

where A is absorbance and ϵ = molar extinction coefficient in $L \text{ mol}^{-1} \text{ cm}^{-1}$.

We found the quantum yield of the TPA in DMF is 0.11 or ~11%.

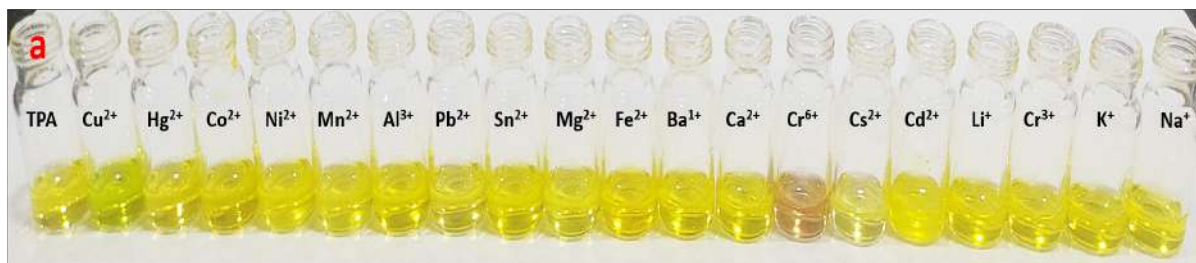


Fig. S25 Vial images of TPA with different metal ions in acetic acid (AcOH). Cr^{6+} is oxidation state in dichromate ions.

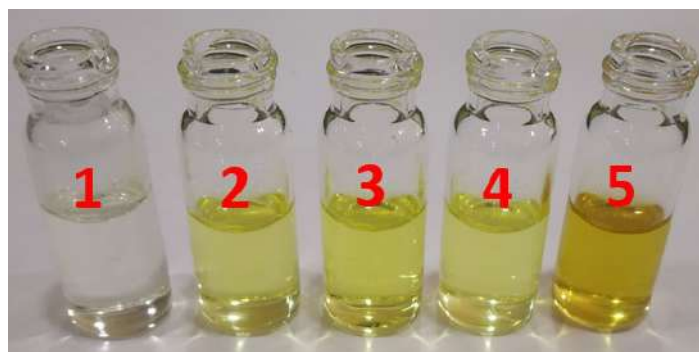


Fig. S26 Vial images TPA (1) in DMSO; (2) in acetic acid (AcOH); (3) TPA in AcOH with F^- ; (4) TPA in AcOH with Cr^{3+} ; (5) TPA in AcOH with $\text{Cr}_2\text{O}_7^{2-}$.

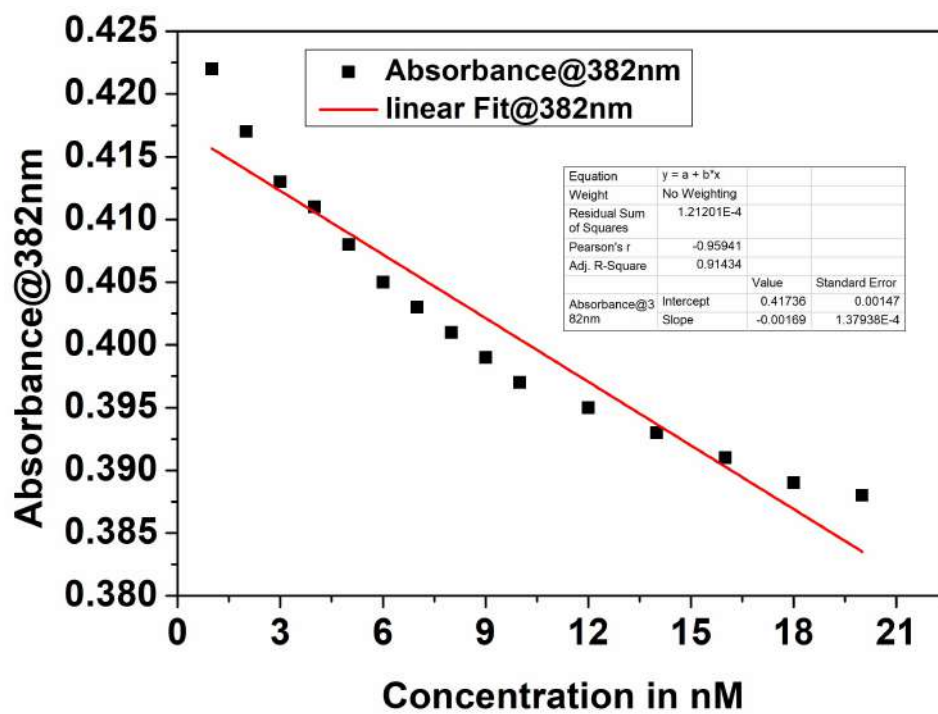


Fig. S27 Limit of detection of (LOD) TPA @ 382 nm

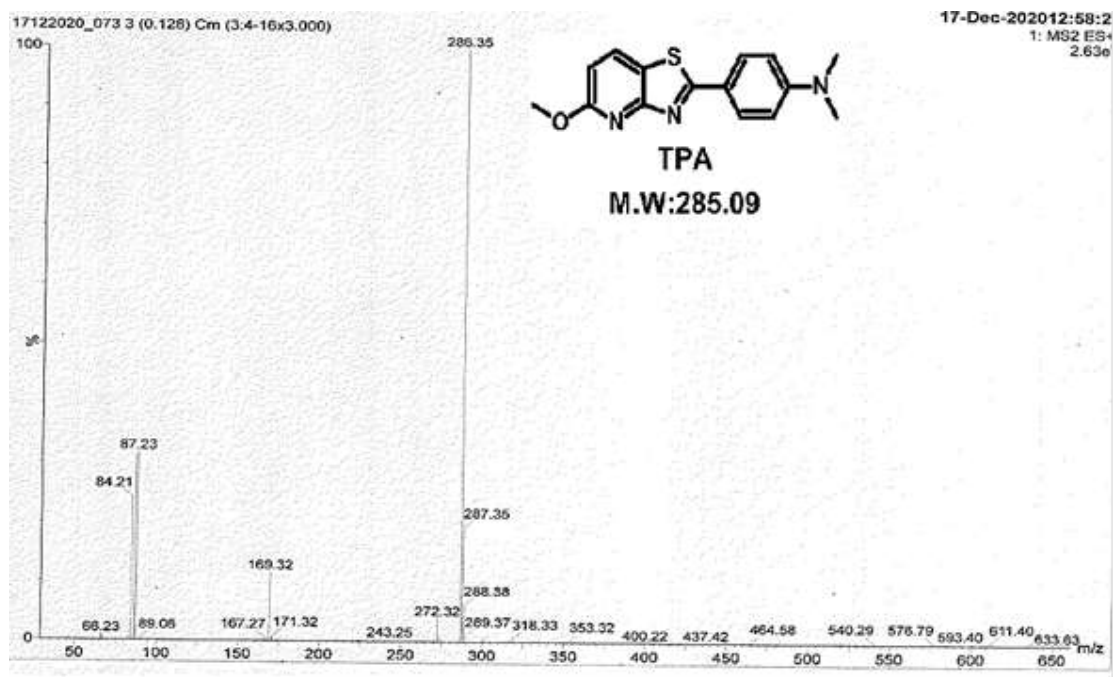


Fig. S28 Mass spectra of TPA

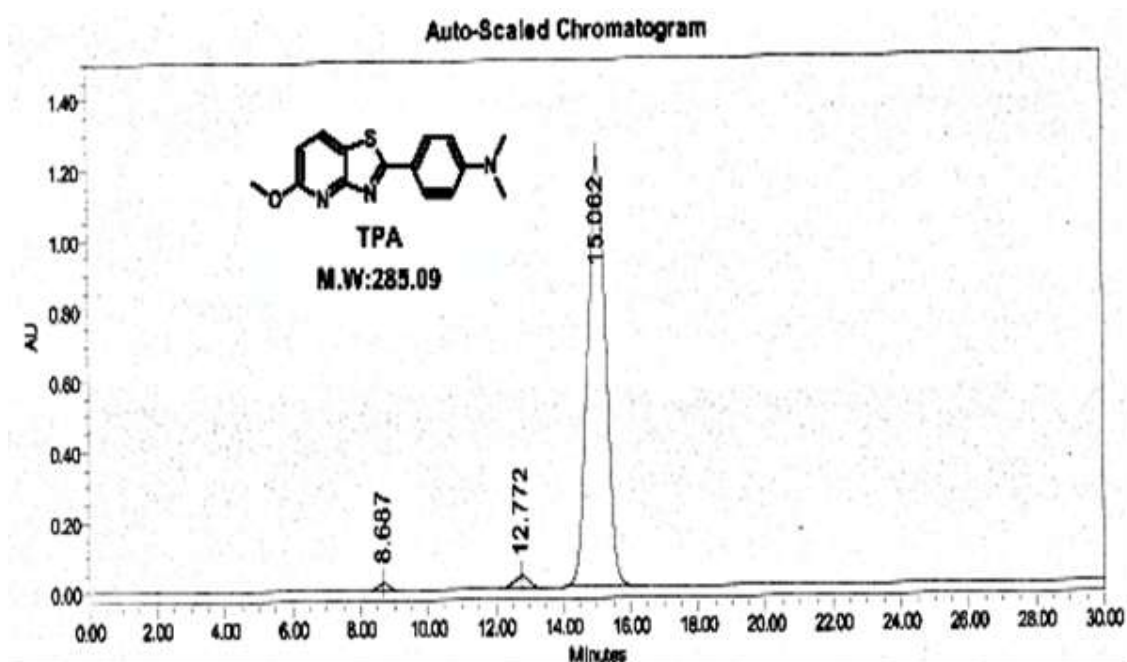


Fig. S29 HPLC Chromatogram of TPA

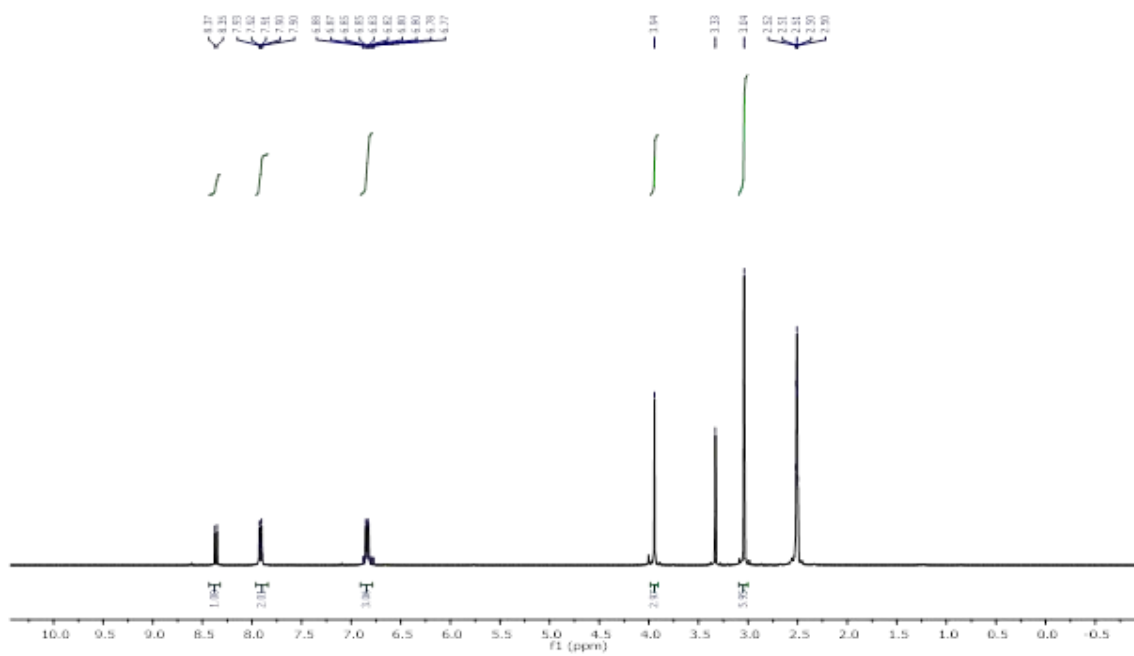


Fig. S30 $^1\text{H-NMR}$ spectra of TPA

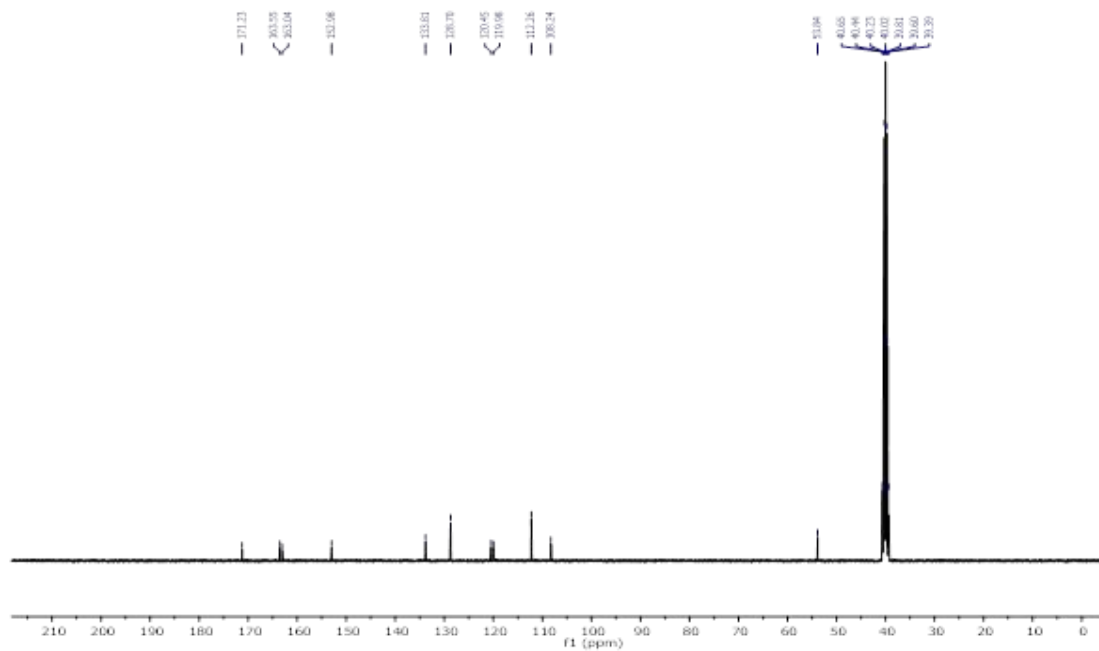


Fig. S31 ^{13}C NMR spectra of TPA

Reference:

- [1] N. Gour, V. Kshtriya, S. Gupta, B. Koshti, R. Singh, D. Patel and K. B. Joshi, *ACS Appl. Bio Mater.*, 2019, **2**, 4442-4455.
- [2] C. Würth, M. Grabolle, J. Pauli, M. Spieles, U. Resch-Genger, *Nat. Protoc.*, 2013, **8**, 1535-1550.
- [3] K. Rurack, M. Spieles, *Anal. Chem.*, 2011, **83**, 1232-1242.